

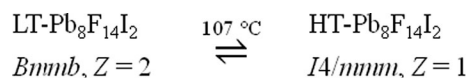
# The phase transition of $\text{Pb}_8\text{F}_{14}\text{I}_2$

Matthias Weil<sup>1</sup> 

Received: 23 August 2016 / Accepted: 3 October 2016 / Published online: 28 October 2016  
© The Author(s) 2016. This article is published with open access at Springerlink.com

**Abstract** The reversible phase transition of  $\text{Pb}_8\text{F}_{14}\text{I}_2$  is of continuous type and takes place at about 107 °C as monitored by temperature-dependent single crystal and powder X-ray diffraction measurements, optical microscopy, and differential scanning calorimetry. The low-temperature ferroelastic phase crystallizes in the orthorhombic crystal system (23 °C,  $Bmmb$ ,  $Z = 2$ ,  $a = 6.0699(6)$  Å,  $b = 6.0165(6)$  Å,  $c = 25.077(2)$  Å, 1487 structure factors, 41 parameter,  $R(F^2) = 0.0346$ ,  $wR(F^2) = 0.0771$ ) and changes its symmetry to the tetragonal crystal system into the high-temperature paraelastic phase (130 °C,  $I4/mmm$ ,  $Z = 1$ ,  $a = 4.2667(12)$  Å,  $c = 25.388(7)$  Å, 430 structure factors, 303 parameter,  $R(F^2) = 0.0575$ ,  $wR(F^2) = 0.1564$ ). Group–subgroup relationships between the two structures and a hypothetical intermediate structure are presented.

*Graphical abstract*



**Keywords** Lead fluoride halide · Crystal structure determination · Thermal analysis · Group–subgroup relationships

## Introduction

In the pseudo-binary system  $\text{PbF}_2/\text{PbI}_2$ , the phases  $(\text{PbF}_2)_7(\text{PbI}_2)$ ,  $(\text{PbF}_2)_5(\text{PbI}_2)$ , and  $(\text{PbF}_2)_4(\text{PbI}_2)$  have been synthesized in the form of single crystals and their crystal structures reported by Aurivillius [1]. Synthesis and unit cell parameter of polycrystalline matlockite-type [2, 3]  $\text{PbFI}$  have been described by Rulmont [4] and Aurivillius [5]; the crystal structure of the latter phase was refined afterwards from single crystal data [6].

The crystal structure of  $(\text{PbF}_2)_7(\text{PbI}_2)$  has originally been determined by Aurivillius on the basis of integrated room temperature Weissenberg data in the orthorhombic space group  $Bmmb$  (standard setting  $Cmcm$ , No. 63) with lattice parameters  $a = 6.0711(6)$  Å,  $b = 6.0198(5)$  Å, and  $c = 25.084(2)$  Å [1]. For that purpose single crystals were originally grown by boiling and recrystallizing a sample with nominal composition of  $10\text{PbF}_2\cdot\text{PbI}_2$  in water. The author reported a systematic twinning of the very tiny and thin crystals in the way that the  $a$ - and  $b$ -axes are interchanged. Due to the method of data collection, the platy crystal form and clearly visible twinning of the investigated single crystal, a straightforward structure refinement was hampered at that time, and the reliability index of 0.109 based on  $|F|$  was rather high. However, all atomic positions could be derived, and for Pb and I atoms anisotropic temperature factors were considered in the final model. The nearly equal lengths of the  $a$ - and  $b$ -axes and an  $I$ -centred pseudo-tetragonal subcell make it appear likely that a phase transition from the room-temperature modification (low-temperature (LT) phase) into a tetragonal high-temperature modification (high-temperature (HT) phase) occurs. Although the author of the original study has theoretically derived an idealized structure model in space group  $I4/mmm$  with the unit cell relations:  $a_{\text{ideal}} \approx (a_{\text{LT}} + b_{\text{LT}})/$

✉ Matthias Weil  
matthias.weil@tuwien.ac.at

<sup>1</sup> Division of Structural Chemistry, Institute for Chemical Technologies and Analytics, TU Wien, Getreidemarkt 9/164-SC, 1060 Vienna, Austria

$\sqrt{8}$ ;  $c_{\text{ideal}} \approx c_{\text{LT}}$ , neither experimental details regarding a possible phase transition nor structure data of the assumed high-temperature phase were reported at that time or afterwards. Therefore, a more detailed examination of a possible phase transition and a redetermination of the crystal structure of  $(\text{PbF}_2)_7(\text{PbI}_2)$  ( $= \text{Pb}_8\text{F}_{14}\text{I}_2$ ) seemed worthwhile.

In this article preparation, ferroelastic behaviour, phase transition and crystal structures of  $\text{Pb}_8\text{F}_{14}\text{I}_2$  at room temperature (LT modification) and at 130 °C (HT modification) as well as their relationships are reported.

## Results and discussion

### Phase transition

Examination of  $\text{Pb}_8\text{F}_{14}\text{I}_2$  (LT) single crystals under a microscope in transmitted polarized light revealed clearly visible multiple domains for most of the crystals, in accordance with the observations by Aurivillius [1]. The domain crystals show ferroelastic behaviour [7] and can be partially or completely reorientated by application of stress with a pair of tweezers along the diagonal or parallel to the  $a$ - or  $b$ -axes (in the setting of space group  $Bmmb$ ). By heating single crystals in inert silicon oil on a Kofler heating stage, a spontaneous change from a biaxial to an uniaxial crystal system in terms of the change of the birefringence of crystal faces was observed at 107(2) °C, indicating a phase transition from the orthorhombic to the tetragonal crystal system. This process was reversible and showed virtually no hysteresis. The observed transition temperatures are in good agreement with a complementary DSC measurement, with on-set temperatures of 104.6 °C (heating; endothermic effect) and 104.0 °C (cooling; exothermic effect) (Fig. 1).

The temperature-dependence of the unit cell parameters for the LT- and HT-phases, as evidenced by X-ray diffraction measurements, is given in Fig. 2. The derived transition temperature of the diffraction experiments is somewhat higher (118(8) °C) for this kind of measurement than those from the optical examinations or DSC measurements. This behaviour is ascribed to the more inaccurate temperature measurement during the diffraction studies where the temperature sensing device was displaced a couple of millimetres from the actual sample. Given the different temperature sensing for the three methods, the derived transition temperature from the DSC experiment appears to be that with the highest accuracy.

The evolution of the orthorhombic unit cell parameters  $a$  and  $b$  (Fig. 2a) reveals a more obvious change of  $a$  towards the transition point than that of  $b$ . The  $c$  unit cell parameter appears not to be directly involved in the

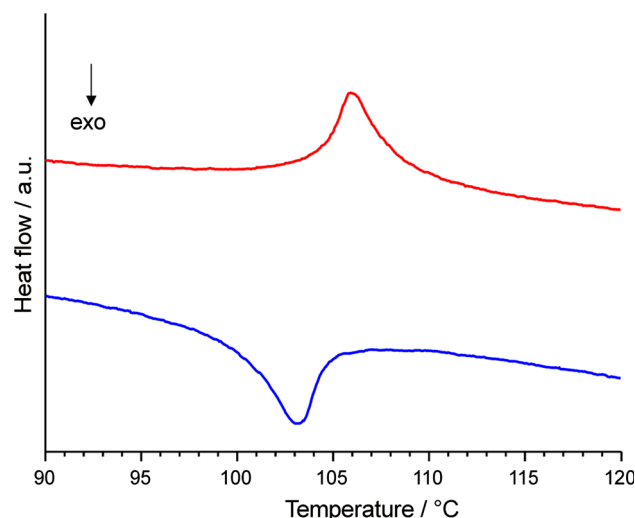


**Fig. 1** DSC curves obtained during heating (red) and cooling (blue) of  $\text{Pb}_8\text{F}_{14}\text{I}_2$  (colour figure online)

transition mechanism (Fig. 2b), with a non-linear behaviour for the temperature-dependence of the LT-phase and a linear behaviour for the HT-phase. The resulting change of the cell volume with temperature is depicted in Fig. 2c. The ratio  $(a - b)/(a + b)$ , where  $a$  and  $b$  are the lengths of the orthorhombic unit cell at a given temperature, is a suitable order parameter  $\eta$  for classification of the type (continuous, discontinuous) of the phase transition. The development of the temperature-dependence of  $\eta = (a - b)/(a + b)$  is given in Fig. 2d and indicates a continuous phase transition from orthorhombic to tetragonal symmetry upon heating. This classification is supported by the continuous change of the unit cell volume with temperature close to the transition point and the observation of the very slight hysteresis observed during optical examination of crystals at the Kofler stage in polarized light or in the DSC curve (Fig. 1) during heating and cooling above and below the transition point.

Above the transition temperature  $\text{Pb}_8\text{F}_{14}\text{I}_2$  is tetragonal, representing the paraelastic phase in space group  $I4/mmm$ ; below the transition temperature it is orthorhombic, representing the ferroelastic phase in space group  $Bmmb$ . There is no direct group-subgroup relation between these two space groups [8, 9], because  $Bmmb$  (or in its standard setting  $Cmcm$ ) is not a maximal subgroup but a general subgroup of  $I4/mmm$  with  $Fmmm$  being the intermediate space group type. The group-subgroup relationships of the paraelastic (HT) and ferroelastic (LT) structures of  $\text{Pb}_8\text{F}_{14}\text{I}_2$ , together with the hypothetical intermediate structure model in  $Fmmm$ , are presented in the form of a Bärnighausen family tree [10] in Fig. 3.

The symmetry reduction from  $I4/mmm$  to  $Fmmm$  is of *translationengleiche* (t) kind with an index of 2, accompanied by a loss of the fourfold rotation axes present in the

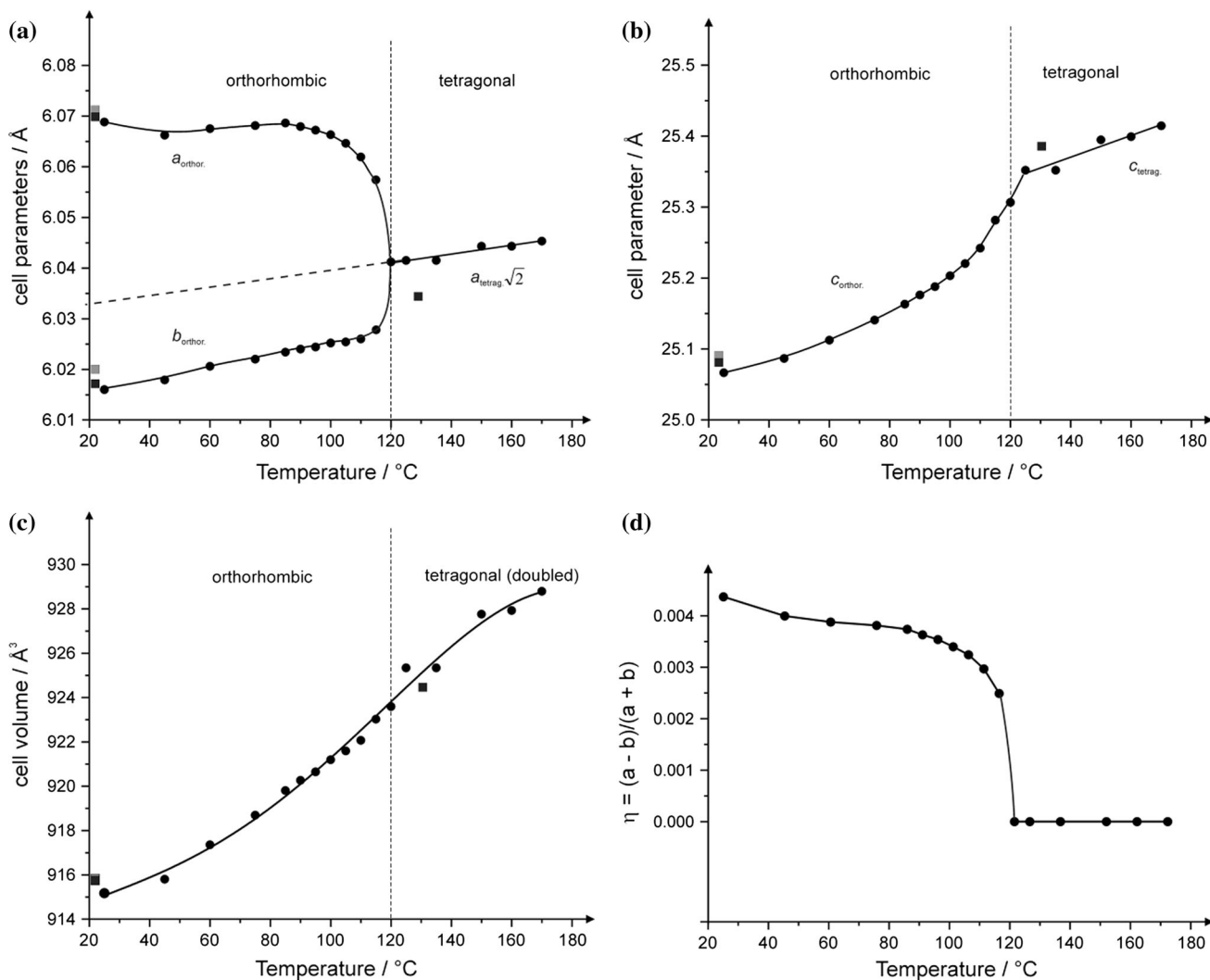


**Fig. 2** Evolution of unit cell parameters of  $\text{Pb}_8\text{F}_{14}\text{I}_2$  with temperature. The crystal has tetragonal symmetry at  $T > T_C$  and orthorhombic symmetry at  $T < T_C$ , with  $a > b$ ; single crystal diffraction data from Aurivillius (grey squares) [1], current single crystal diffraction data (black squares), powder X-ray diffraction data (black circles); the size of the symbols is greater than the standard deviation

higher-symmetry structure. The relationship between the  $Fm\bar{3}m$  structure and  $Bm\bar{3}b$  is of *klassengleiche* (k) kind with an index of 2 under change of the Bravais centering from  $F$  to  $B$ . The first *translationengleiche* transition of index 2 from  $I4/m\bar{3}m \rightarrow Fm\bar{3}m$  is a ferroic transition [11] and explains the presence of two twin domains in the resulting crystals of the LT- $\text{Pb}_8\text{F}_{14}\text{I}_2$  polymorph.

### Structure description: LT-phase

The current structure refinement confirms the original model [1]; however, with increased precision and accuracy. The crystal structure is made up of four-layer “ $\text{PbF}_2$ ”-type blocks

of individual values.  $a$  and  $b$  axes (the identical unit cell parameters  $a$  and  $b$  in the tetragonal HT-phase can be extrapolated into the temperature interval of the orthorhombic LT-phase, *dashed line*);  $c$  axis; **c** volume; **d** plot of the temperature-dependent course of the order parameter  $\eta$  of  $\text{Pb}_8\text{F}_{14}\text{I}_2$

consisting of four unique  $\text{Pb}^{2+}$  cations. The blocks are stacked along [001] with a mean Pb–F distance of 2.63 Å which is in good agreement with the sum of the ionic radii [12] for  $\text{Pb}^{2+}$  and  $\text{F}^-$  (2.60 Å; weighted according to the different coordination numbers as discussed below). The “ $\text{PbF}_2$ ”-type blocks are separated by interstitial  $\text{I}^-$  ions that are located at  $z \approx 1/4$  and  $3/4$  (Fig. 4, left) with a mean Pb–I distance of 3.70 Å. The “ $\text{PbF}_2$ ”-type blocks contain additional ordered  $\text{F}^-$  ions (F1) with one close contact of 2.261(10) Å to Pb2. The latter defines one of the boundaries of the blocks and is additionally bonded to the interstitial  $\text{I}^-$  ions. Due to the additional F1 ions, the coordination numbers (CN) of the central  $\text{Pb}^{2+}$  cations in each block are increased in comparison with fluorite-type  $\text{PbF}_2$  (CN = 8), to

**Fig. 3** Group–subgroup relations for the HT- and LT-forms of  $\text{Pb}_8\text{F}_{14}\text{I}_2$  and the hypothetical intermediate phase in  $Fmmm$ . Coordinates of HT- and LT- $\text{Pb}_8\text{F}_{14}\text{I}_2$  refer to the refined coordinates (deposited as CIFs, see *Experimental*) but here due to truncation with somewhat lower precision

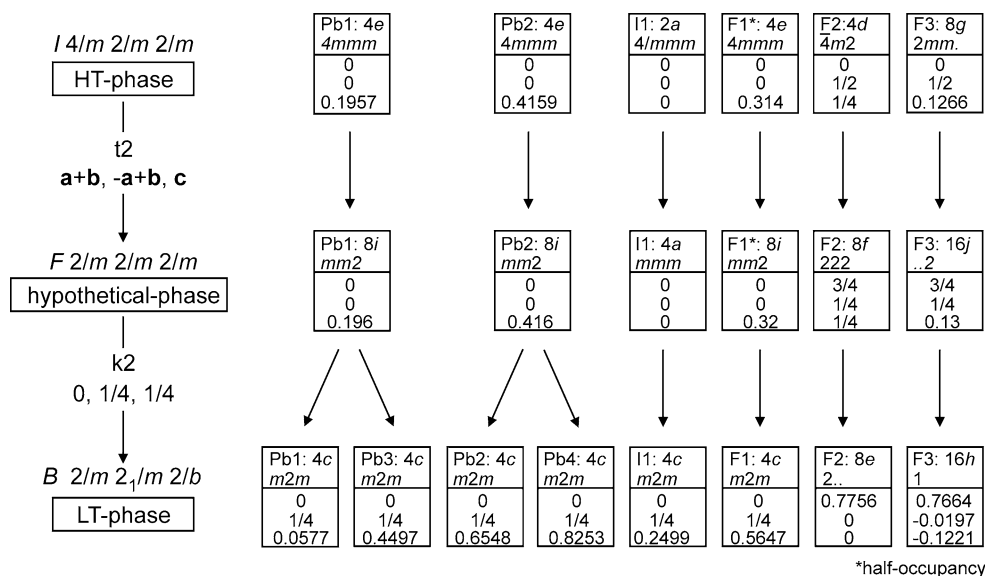
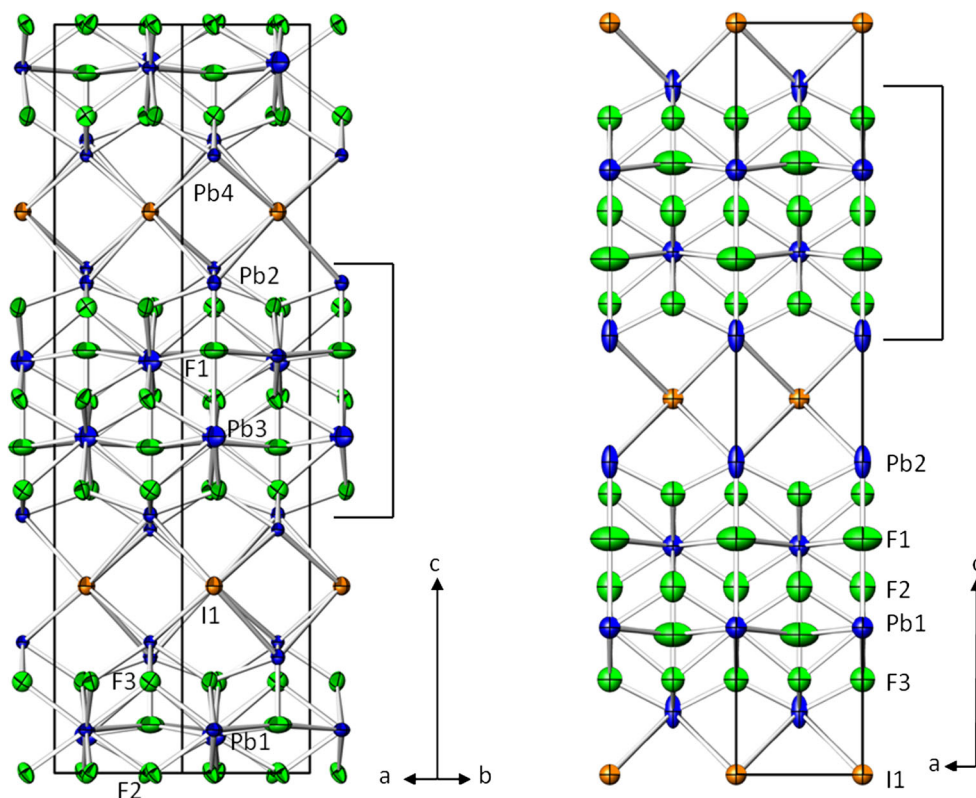


**Fig. 4** The crystal structures of  $\text{Pb}_8\text{F}_{14}\text{I}_2$  in the LT-(left) and HT-(right) modifications, with projections along [110] and [010], respectively. Anisotropic displacement parameters are drawn at the 74% probability level. The *right brackets* designate the “ $\text{PbF}_2$ ”-type blocks in the structure



CN = 10 for Pb1 (resulting coordination polyhedron: bicapped cube) and CN = 11 (tricapped cube) for Pb3. The terminal  $\text{Pb}^{2+}$  cations at the boundaries of the blocks exhibit CN = 9 for Pb2 (four  $\text{I}^-$  and four  $\text{F}^-$  ions plus one capping  $\text{F}^-$ ; distorted monocapped square antiprism), and CN = 8 for Pb4 (four  $\text{I}^-$  and four  $\text{F}^-$  ions; distorted square antiprism). All Pb–F and Pb–I bond lengths (Table 2) are comparable with those of matlockite-type  $\text{PbFI}$  [6] or the other structures in the system  $\text{PbF}_2/\text{PbI}_2$  [1].

#### HT-phase

In the structure of the HT-phase (Fig. 4, right) only two unique  $\text{Pb}^{2+}$  cations are present; the interstitial F1 atom now shows half-occupancy. The central  $\text{Pb}^{2+}$  cation (Pb1) of the “ $\text{PbF}_2$ ”-type block has CN = 11 (tricapped cube) and the terminal  $\text{Pb}^{2+}$  cation (Pb2) has CN = 9 (four  $\text{I}^-$  and four  $\text{F}^-$  ions plus one capping  $\text{F}^-$ ; monocapped square antiprism). In comparison with the structure of the LT-

**Table 1** Details of single crystal X-ray data collections and structure refinements

| Phase  | $\text{Pb}_8\text{F}_{14}\text{I}_2$ (LT) | $\text{Pb}_8\text{F}_{14}\text{I}_2$ (HT) |
|--|---|---|
| Temperature/ $^{\circ}\text{C}$                                    | 23  | 130                                       |
| $M_r$  | 2177.32                                   |   |
| Crystal size/ $\text{mm}^3$  | $0.015 \times 0.100 \times 0.100$         |   |
| Crystal colour, form   | Colourless, plate                         |   |
| Crystal system   | Orthorhombic                              | Tetragonal                                |
| Space group, no.   | <i>Bmmb</i> , 63                          | <i>I4/mmm</i> , 139                       |
| $a/\text{\AA}$   | 6.0699(6)                                 | 4.2667(12)                                |
| $b/\text{\AA}$   | 6.0165(6)                                 |   |
| $c/\text{\AA}$   | 25.077(2)                                 | 25.388(7)                                 |
| $V/\text{\AA}^3$   | 915.80(16)                                | 462.2(3)                                  |
| $Z$  | 2   | 1   |
| $D_{\text{calcd}}/\text{g cm}^{-3}$                                | 7.896                                     | 7.823                                     |
| $\mu(\text{MoK}\alpha)/\text{mm}^{-1}$                             | 76.864                                    | 76.027                                    |
| Theta range/ $^{\circ}$  | 1.624–38.733                              | 3.210–37.513                              |
| $hkl$ range  |   |   |
| $h$  | –10 to 10                                 | –7 to 7                                   |
| $k$  | –10 to 10                                 | –7 to 7                                   |
| $l$  | –44 to 43                                 | –42 to 43                                 |
| Reflections measured   | 34113                                     | 15499                                     |
| Reflections unique   | 1487                                      | 430                                       |
| Reflections [ $I > 2\sigma(I)$ ]                                   | 956                                       | 303                                       |
| $R_{\text{int}}$   | 0.1396                                    | 0.1091                                    |
| Extinction coefficient   | 0.00023(2)                                | 0.0008(3)                                 |
| Twin ratio   | 0.507:0.493                               |   |
| Parameters refined   | 41  | 19  |
| $R(F^2)/wR(F^2)$ [ $I > 2\sigma(I)$ ]                              | 0.0346/0.0689                             | 0.0575/0.1420                             |
| $R(F^2)/wR(F^2)$ [all reflections]                                 | 0.0695/0.0771                             | 0.0864/0.1564                             |
| Goof ( $F^2$ )   | 0.895                                     | 1.189                                     |
| $\Delta\rho_{\text{fin}}$ (max/min)/ $\text{e}^{-}\text{\AA}^{-3}$ | 5.106/–5.602                              | 4.401/–9.657                              |
| CSD number   | 431846                                    | 431847                                    |

phase, the mean Pb–F distance in the “ $\text{PbF}_2$ ”-type blocks slightly increases to 2.70 Å, whereas the mean Pb–I distance of the LT-phase and that of the HT-phase are more or less the same. Comparison of the individual Pb–F and Pb–I bond lengths reveals a shift of individual atoms up to 0.25 Å for the lighter F and 0.15 Å for heavy I atoms.

## Experimental

### Preparation

Single crystals of  $\text{Pb}_8\text{F}_{14}\text{I}_2$  were grown under hydrothermal conditions from stoichiometric amounts of  $\text{PbI}_2$  (Riedel-de Haën, pure) and  $\text{PbF}_2$  (Aldrich, 99 + %). The starting materials were homogenized by grinding and placed in a 5-cm<sup>3</sup> Teflon® container that was filled up to two-thirds of its volume with

demineralized water. The Teflon® container was then closed and placed in a steel autoclave and subjected to the following heating protocol: 25 → 250 °C [2 h], 250 °C [10 days], 250 → 25 °C [10 h]. Nearly colourless laminated crystals of  $\text{Pb}_8\text{F}_{14}\text{I}_2$  and few very thin crystals with a plate-like form and light-yellow colour of  $\text{PbFI}$  [6] were obtained. Microcrystalline samples of  $\text{Pb}_8\text{F}_{14}\text{I}_2$  were prepared by reaction of stoichiometric amounts of  $\text{PbF}_2$  and  $\text{PbI}_2$  in sealed and evacuated silica ampoules at 380 °C for 1 week.

### DSC measurements

DSC measurements were performed with ~20 mg samples on a NETZSCH DSC 200F3 system in the temperature range 30–150 °C (aluminium crucibles with pierced lid, flowing argon atmosphere (20 cm<sup>3</sup>/min), heating rate 5 °C min<sup>–1</sup>).

**Table 2** Selected bond lengths/Å

| Pb <sub>8</sub> F <sub>14</sub> I <sub>2</sub> (LT) |            |    | Pb <sub>8</sub> F <sub>14</sub> I <sub>2</sub> (HT) |            |    |
|---|------------|----|---|------------|----|
| Pb1–F2  | 2.492(5)   | 4× | Pb1–F2  | 2.5404(9)  | 4× |
| Pb1–F3  | 2.693(6)   | 4× | Pb1–F3  | 2.762(11)  | 4× |
| Pb1–F1  | 3.0400(7)  | 2× | Pb1–F1  | 3.00(6)    |    |
| Pb2–F1  | 2.261(10)  |    | Pb1–F1  | 3.027(5)   | 4× |
| Pb2–F3  | 2.434(5)   | 4× | Pb2–F3  | 2.390(8)   | 4× |
| Pb2–I1  | 3.8415(9)  | 2× | Pb2–F1  | 2.59(6)    |    |
| Pb2–I1  | 3.8594(9)  | 2× | Pb2–I1  | 3.6967(14) | 4× |
| Pb3–F2  | 2.579(6)   | 4× |   |            |    |
| Pb3–F3  | 2.789(6)   | 4× |   |            |    |
| Pb3–F1  | 2.884(10)  |    |   |            |    |
| Pb3–F1  | 3.0298(13) | 2× |   |            |    |
| Pb4–F3  | 2.381(5)   | 4× |   |            |    |
| Pb4–I1  | 3.5504(8)  | 2× |   |            |    |
| Pb4–I1  | 3.5756(8)  | 2× |   |            |    |

### X-ray diffraction and single crystal structure analysis

Polycrystalline samples were characterized by X-ray powder diffraction with CuK<sub>α1,2</sub> radiation ( $\lambda = 1.54060$ ,  $1.54439$  Å). At room temperature a Philips X'pert system was used. Temperature-dependent measurements were performed on a Philips PW1012/10 diffractometer equipped with a home-built heat controlling system. Unit cell parameters were refined with the program TOPAS [13].

Single crystal X-ray data were collected on a Bruker APEX II CCD diffractometer with MoK<sub>α</sub> radiation ( $\lambda = 0.71079$  Å). For single crystal X-ray measurements at room temperature, optically controlled single domain crystals of Pb<sub>8</sub>F<sub>14</sub>I<sub>2</sub> (RT, 23 °C) were fixed with cyanoacrylate adhesive on thin silica glass fibres. For high-temperature measurement of Pb<sub>8</sub>F<sub>14</sub>I<sub>2</sub> (HT, 130 °C), a more temperature-resistant two-component adhesive was used. Heating was provided with a gas-flow heater using a stream of nitrogen. Diffraction data for the two measurements were corrected for absorption effects with the program HABITUS [14]. Full-matrix least-squares refinements on  $F^2$  for the two data sets and correction of extinction effects were carried out with the program SHELXL-2014 [15].

For the LT-phase the coordinates of the reported structure model [1] were taken as starting parameters for refinement in the space group *Bmmb*. The measured crystal was twinned by pseudo-merohedry with a rotation by 90° along [001] as twin element (refined twin ratio of the twin domains 1:1). For the HT-phase the proposed coordinates of the idealized structure model [1] in the space group *I4/mmm* were used. For the two models anisotropic displacement parameters for all atoms were refined.

Details of data collections and structure refinements are listed in Table 1. Selected bond lengths are collated in Table 2. Further details of the crystal structure investigations may be obtained from Fachinformationszentrum Karlsruhe, 76344 Eggenstein-Leopoldshafen, Germany (fax: (+49)7247-808-666; e-mail: crysdata@fiz-karlsruhe.de, <https://www.fiz-karlsruhe.de/icsd.htm>) on quoting the appropriate CSD number listed at the end of Table 1. Drawings of structural details were produced using the program ATOMS [16].

**Acknowledgements** Open access funding provided by TU Wien (TUW). The X-ray centre of TU Wien is acknowledged for providing access to the single crystal and powder diffractometers.

**Open Access** This article is distributed under the terms of the Creative Commons Attribution 4.0 International License (<http://creativecommons.org/licenses/by/4.0/>), which permits unrestricted use, distribution, and reproduction in any medium, provided you give appropriate credit to the original author(s) and the source, provide a link to the Creative Commons license, and indicate if changes were made.

### References

1. Aurivillius B (1980) Chem Scripta 15:153
2. Nieuwenkamp W, Bijvoet JM (1932) Z Kristallogr 81:469
3. Pasero M, Perchiazzi N (1996) Mineral Mag 60:833
4. Rulmont A (1973) CR Acad Sci Ser C 276:775
5. Aurivillius B (1976) Chem Scripta 10:206
6. Weil M, Kubel F (2001) Acta Crystallogr E57:i80
7. Salje EKH (1990) Phase transitions in ferroelastic and co-elastic crystals. Cambridge University Press, Cambridge
8. Ivantchev S, Kroumova E, Madariaga G, Perez-Mato JM, Aroyo MI (2000) J Appl Crystallogr 33:1190
9. Müller U (2013) Symmetry relationships between crystal structures. Oxford University Press, Oxford

10. Bärnighausen H (1980) MATCH 9:139
11. Wadhawan VK (2006) Phase Transitions 64:165
12. Shannon RD (1976) Acta Crystallogr A 32:751
13. Bruker-AXS (2012) TOPAS 4.2. Bruker-AXS, Karlsruhe
14. Herrendorf W (1997) HABITUS. University of Gießen, Germany
15. Sheldrick GM (2015) Acta Crystallogr C 71:3
16. Dowty E (2008) ATOMS for Windows. Shape Software, Kingsport